# Search for the Rare Decays $K_L^0 \to \mu e$ and $K_L^0 \to ee$

T. Akagi,[1] R. Fukuhisa,[2] Y. Hemmi,[3] T. Inagaki,[4] K. Ishikawa,[2],[a] T. Kishida,[2] M. Kobayashi,[4] T. K. Komatsubara,[2] M. Kuze,[2],[b] F. Sai,[2],[c] T. Sato,[4] T. Shinkawa,[4] F. Suekane,[4],[d] K. Takamatsu,[4] J. Toyoura,[2],[e] S. S. Yamamoto,[2] and Y. Yoshimura[4]

[1]*Department of Physics, Tohoku University, Sendai 980, Japan*
[2]*Department of Physics, University of Tokyo, Tokyo 113, Japan*
[3]*Department of Physics, Kyoto University, Kyoto 606, Japan*
[4]*National Laboratory for High Energy Physics (KEK), Tsukuba 305, Japan*

(Received 22 July 1991)

A search for the rare decays $K_L^0 \to \mu e$ and $K_L^0 \to ee$ was performed at the KEK 12-GeV Proton Synchrotron. No event was observed in the fiducial region for the decay $K_L^0 \to \mu e$. There was one event in the fiducial region for the decay $K_L^0 \to ee$, which was indistinguishable from the background. The upper limits on the branching ratios at 90% confidence level were $B(K_L^0 \to \mu e) < 9.4 \times 10^{-11}$ and $B(K_L^0 \to ee) < 1.6 \times 10^{-10}$.

PACS numbers: 13.20.Eb

The decay $K_L^0 \to \mu e$ is a lepton-flavor-changing process that is forbidden by the standard model with massless neutrinos. Even in the minimal extension model which introduces an experimentally allowed finite neutrino mass and mixing among leptons like among quarks, the process is highly suppressed [1] due to the smallness of the neutrino mass. Therefore, the decay $K_L^0 \to \mu e$ provides a good means to search for new interactions [1,2], such as the left-right symmetric model, new interactions among generations, and the technicolor model. The decay $K_L^0 \to ee$ is allowed by the standard model, but it is much more suppressed than the decay $K_L^0 \to \mu\mu$ due to the muon-electron mass difference. The branching ratio of the decay $K_L^0 \to ee$ is predicted to be $(3\text{-}5) \times 10^{-12}$ [3]. The sensitivity of this experiment for the decays $K_L^0 \to \mu e$ and $K_L^0 \to ee$ is about $4 \times 10^{-11}$ and better than those previously achieved [4-7].

The experiment was carried out using the K0 beam line of the KEK 12-GeV Proton Synchrotron (PS). A neutral beam was taken at 0° with respect to the primary proton beam for the first three quarters of the running period, and at 2° for the last quarter period. The beam was collimated into a cone (154 $\mu$sr) by two brass collimators having a half-cone angle of 7 mrad. The average intensity of the primary proton beam impinging on a 120-mm-long copper target was about $1.2 \times 10^{12}$ protons per pulse (ppp) for the 0° production and $2.0 \times 10^{22}$ ppp for the 2° production. A 10-m-long vacuum chamber was located at 10.5 m from the target and was evacuated to better than 0.4 Torr. Figure 1 shows a plan view of the detector system whose major features were described elsewhere [7]. A beam pipe which was connected to the vacuum chamber was placed along the central line of the double-arm detector for transmitting the neutral beam. Each arm of the detector consisted of five drift chambers $W1$-$W5$, two dipole magnets, two hodoscopes $H1$ and

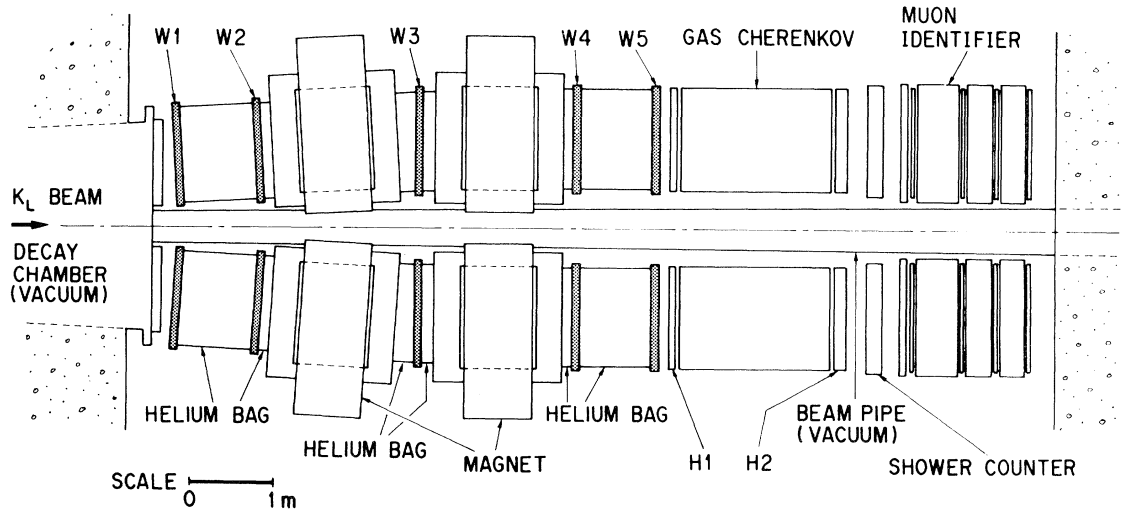


FIG. 1. Plan view of the detector system.

$H2$, a gas Cherenkov counter, an electromagnetic shower counter, and a muon identifier. To reduce the material in the upstream part of the detector up to $W5$, two exit windows of the vacuum chamber were made of thin film (50-$\mu$m-thick polyester film supported by 60-mg/cm$^2$ carbon cloth) and helium bags were placed between drift chambers. Each drift chamber had four sense-wire planes $X$, $X'$, $Y$, and $Y'$, where the $X'$ and $Y'$ planes were staggered by a half cell size with respect to the $X$ and $Y$ planes, respectively. The two identical dipole magnets were equally excited to have an integrated field strength of 0.79 Tm in each arm. It corresponded to a transverse-momentum kick of 238 MeV/$c$, so that the acceptance for three-body decays such as the $K_{l3}$ decays could be efficiently reduced, while maintaining relatively large acceptances for the two-body decays by requiring that the particles should be parallel to the $K_L^0$ direction at the hodoscopes. The radiator of the gas Cherenkov counter was air at atmospheric pressure whose threshold momentum for muons was 4.5 GeV/$c$. The electromagnetic shower counter was made of ten alternate layers of 6-mm-thick plastic scintillators and 8-mm-thick lead sheets. The muon identifier consisted of four iron blocks with thicknesses of 10, 50, 30, and 30 cm, each of which was followed by a scintillator hodoscope.

The basic trigger was a coincidence between an $H1$ counter and the corresponding $H2$ counter in both arms. For the $K_L^0 \rightarrow \mu e$, $ee$, and $\mu\mu$ [8] triggers, additional lepton-identifier signals for muons and/or electrons were required. The muon signal was made by a matrix coincidence between counters in the first two hodoscopes of the muon identifier, which corresponded to the requirement that the momentum of the muon should be above 1.0 GeV/$c$. For the electron a signal corresponding to more than one photoelectron in the gas Cherenkov counter and a signal corresponding to the electron energy above 500 MeV in the electromagnetic shower counter were required. For the 2° production run the requirement of the electromagnetic shower counter was removed. The trigger for the decay $K_L^0 \rightarrow \pi^+\pi^-$ was made only by the hodoscopes without particle identification. Since the pions from the decay $K_L^0 \rightarrow \pi^+\pi^-$ were bent slightly inward, the $H1$-$H2$ coincidence requirement mentioned above was relaxed so that either the coincidence between an $H1$ counter and the corresponding $H2$ counter or the adjacent one on the beam pipe side was required. This trigger was prescaled typically by a factor of 500. No veto was required for any of the triggers. The four decay modes, $K_L^0 \rightarrow \mu e$, $ee$, $\mu\mu$, and $\pi^+\pi^-$, were simultaneously triggered and tagged. The total trigger rate was less than 100 per beam pulse. The dead time due to the inhibition of the trigger was around 5% of the data-taking time.

In the off-line analysis track candidates were selected from the hit positions in the drift chambers and the $H1$ and $H2$ hodoscopes in each arm. After fitting hit positions of each track candidate to a bent line, the most probable track candidate was selected. A magnetic-field map extending from $W1$ to $W5$ in each arm was used for fitting hit positions of the track candidate to a smooth track by the spline method. The track $\chi^2$ was calculated using an error matrix for the spectrometer in each arm to check the track fitting quality. For the error matrix the position resolution of the drift chambers (about 300 $\mu$m) and the contribution from multiple Coulomb scattering were taken into account. A nearly flat probability distribution of the track $\chi^2$ was obtained. All tracks with reduced $\chi^2$ ($\chi^2$/degree of freedom) of greater than 4 were rejected. Furthermore, the momenta of a track measured in the upstream and downstream halves of the spectrometer were checked for consistency to reject a particle which had decayed in flight during the passage through the spectrometer. The cut $(|p_u - p| + |p_d - p|)/p < 0.06$ was used for this check, where $p_u$, $p_d$, and $p$ are the momenta measured in the upstream ($W1$-$W3$) and downstream ($W3$-$W5$) halves of the spectrometer and in the whole spectrometer ($W1$-$W5$), respectively. The loss of the genuine track by this cut was estimated to be 7% by a Monte Carlo calculation. Only the tracks which survived these cuts were used in the subsequent analysis. The tracks in both arms were extrapolated in the upstream direction and the point of their closest approach was defined as the decay vertex. The angle $\theta$ between the target-to-vertex direction and the vector sum of the two-track momenta was calculated.

In order to reject the background unassociated with the $K_L^0$ decays, the following cuts were applied to the reconstructed events: (1) The distance between two tracks at the decay vertex had to be less than 1.5 cm; (2) the vertex point had to lie within the vacuum chamber and within a beam cone of less than 250 $\mu$sr; (3) the momentum of each track had to be less than 4.5 GeV/$c$; and (4) the ratio of the momentum of one track to that of the other had to be within the range between $\frac{1}{3}$ and 3. These cuts were loose enough to pass more than 99% of the genuine events, and their effect on the relative efficiency of the leptonic modes to the $\pi^+\pi^-$ mode was negligibly small, as indicated by a Monte Carlo calculation.

For the purpose of particle identification of the tracks, they were extrapolated in the downstream direction to search for hits in the particle-identification counters. The responses of these counters to pions, muons, and electrons were calibrated by using well-identified particles from samples of the $K_{l3}$ decays in the $\pi^+\pi^-$ triggered data. The muon requirement was based on the range-momentum relation using the four layers of hodoscopes in the muon identifier. For an electron a signal of at least two photoelectrons in the gas Cherenkov counter and the energy deposit in the electromagnetic shower counter of more than 0.7 times its momentum were required. Muon identification was made by the presence of a proper signal in the muon identifier and the absence of a proper electron signal in both the electromagnetic shower counter and the gas Cherenkov counter. Electron identification was made by the presence of a proper signal in both the

electromagnetic shower counter and the gas Cherenkov counter and the absence of a proper muon signal in the muon identifier. The pion was identified by the absence of a proper signal in both the gas Cherenkov counter and the muon identifier. The efficiency of the muon identifier and that of the electromagnetic shower counter were determined as a function of particle momentum, and that of the gas Cherenkov counter was determined as a function of the hit position. The average particle-identification efficiencies for $\pi^+\pi^-$, $\mu e$, and $ee$ modes were $0.937 \pm 0.003$, $0.744 \pm 0.005$, and $0.730 \pm 0.004$, respectively.

Figure 2(a) shows a scatter plot of the effective mass ($M_{\pi^+\pi^-}$) vs $\theta^2$ for the $\pi^+\pi^-$ events. The fiducial region was defined as $493 < M_{\pi^+\pi^-} < 502$ MeV/$c^2$ and $\theta^2 < 3$ mrad$^2$; the acceptable mass and angular ranges were about 3 times their resolutions. The number of $K_L^0 \rightarrow \pi^+\pi^-$ events was determined by subtracting the number of background events from the number of events in the fiducial region. It was $6.37 \times 10^7$ after correcting for the prescaling factor. The relative acceptances of the same fiducial region for the $\mu e$ and $ee$ modes with respect to the $\pi^+\pi^-$ mode were $0.939 \pm 0.009$ and $0.940 \pm 0.009$, respectively. The average loss due to nuclear interaction in the detector for the decay $K_L^0 \rightarrow \pi^+\pi^-$ was $0.057 \pm 0.006$. The correction for a different dead-time effect on the $\pi^+\pi^-$ mode from the leptonic modes was $(1.3 \pm 0.3)\%$. By using the $K_L^0 \rightarrow \pi^+\pi^-$ branching ratio [4] of $(2.03 \pm 0.04) \times 10^{-3}$, the single-event sensitivity was calculated to be $(4.08 \pm 0.12) \times 10^{-11}$ for the decay $K_L^0 \rightarrow \mu e$ and $(4.16 \pm 0.13) \times 10^{-11}$ for the decay $K_L^0 \rightarrow ee$. The errors are systematic.

Figure 2(b) shows a scatter plot of the effective mass ($M_{\mu e}$) vs $\theta^2$ for the $\mu e$ events. No event is seen in the fiducial region. Thus the upper limit of the $K_L^0 \rightarrow \mu e$ branching ratio at 90% confidence level which corresponded to the presence of 2.3 events was determined to be $9.4 \times 10^{-11}$ with a systematic error of 3%. The number of background events in the fiducial region expected from the main background source, which is the decay $K_L^0 \rightarrow \pi e \nu$ whose pion has decayed into a muon in the spectrometer and from another source, the double misidentification ($\pi \rightarrow e$ and $e \rightarrow \mu$), for the decay $K_L^0 \rightarrow \pi e \nu$, is negligibly small.

There is one event in the fiducial region in the $ee$ plot as shown in Fig. 2(c). Figure 3(a) shows a plot of $M_{ee}$ vs $p_t$ over an extended mass region, where $p_t$ is the transverse momentum of the $ee$ system with respect to the target-to-vertex direction. There are several high mass events above a cluster of $K_L^0 \rightarrow \pi e \nu$ events whose pion is misidentified as an electron. Figure 3(b) shows a scatter plot of $ee$ events expected from a Monte Carlo calculation which included the decays $K_L^0 \rightarrow \pi e \nu$, $K_L^0 \rightarrow ee\gamma$ [9], and $K_L^0 \rightarrow eeee$ [10] as the background sources for $ee$ events at a 10 times greater sensitivity of this experiment. The general shape of the Monte Carlo–generated event distribution is quite similar to Fig. 3(a), and the high mass

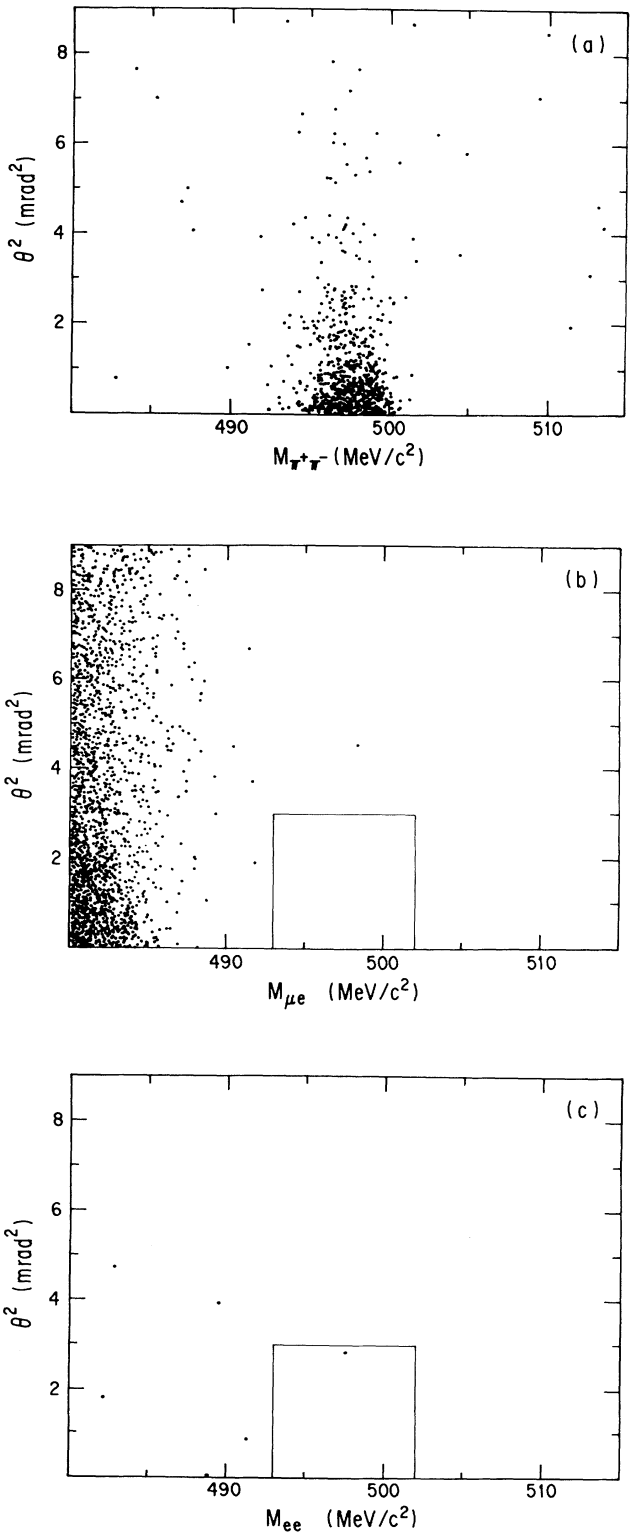


FIG. 2. (a) The $\pi^+\pi^-$ effective mass vs $\theta^2$ plot based on a representative sample of 1000 events; (b) the $\mu e$ effective mass vs $\theta^2$ plot; and (c) the $ee$ effective mass vs $\theta^2$ plot. Boxes indicate the boundary of the fiducial region, $493 < M < 502$ MeV/$c^2$ and $\theta^2 < 3$ mrad$^2$.

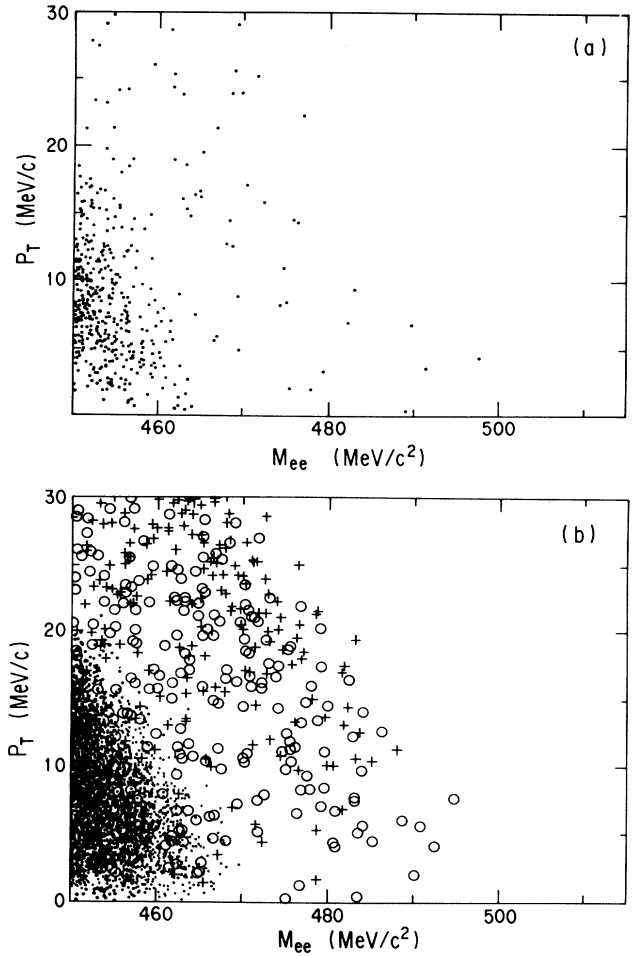


FIG. 3. (a) The $ee$ effective mass vs $p_t$ plot. (b) The $ee$ effective mass vs $p_t$ plot by a Monte Carlo calculation; contribution from the decays $K_L^0 \to \pi e \nu$ (●), $K_L^0 \to ee\gamma$ (+), and $K_L^0 \to eeee$ (○).

events in the actual data seem to come mainly from the decays $K_L^0 \to ee\gamma$ and $K_L^0 \to eeee$, the latter decay mode being mostly responsible for the events in the $M_{ee} > 485$ MeV/$c^2$ region. The decay $K_L^0 \to eeee$ is theoretically predicted [10], and two events have been observed recently [11]. The one event in the fiducial region is at the tail end of the background distribution and cannot be distinguished from it at the level of one-event sensitivity. Therefore, the upper limit of the $K_L^0 \to ee$ branching ratio at 90% confidence level which corresponded to the presence of 3.9 events was determined to be $1.6 \times 10^{-10}$.

We are grateful to the operating crew of the KEK 12-GeV PS and the members of the Beam-Channel and Counter-Hall Groups, the Electronics and On-line Groups, the Computing Center, and the Mechanical Engineering Center at KEK for their indispensable assistance. We express our sincere gratitude to Professor T. Nishikawa, Professor H. Sugawara, Professor K. Nakai, Professor S. Iwata, and the members of the physics departments of KEK, University of Tokyo, Kyoto University, and Tohoku University for their continuous encouragement and support. T.K.K. is a JSPS Fellow for Japanese Junior Scientists.

[a]Present address: 2-2-12, Wakamatsuhigashi, Okazaki 444, Japan.
[b]Present address: Institute for Nuclear Study, University of Tokyo, Tanashi 188, Japan.
[c]Present address: Tokyo Research Laboratory, IBM Ltd., Tokyo 102, Japan.
[d]Present address: Department of Physics, Tohoku University, Sendai 980, Japan.
[e]Present address: Research Laboratory, Mitsubishi Electric Corp., Amagasaki 661, Japan.

[1] P. Langacker, S. U. Sankar, and K. Schilcher, Phys. Rev. D **38**, 2841 (1988).
[2] A. Barroso, G. C. Branco, and M. C. Bento, Phys. Lett. **134B**, 123 (1984); W. S. Hou and A. Soni, Phys. Rev. Lett. **54**, 2083 (1985); J. Ellis, D. V. Nanopoulos, and P. Sikivie, Phys. Lett. **101B**, 387 (1981); S. Dimopoulos, S. Raby, and G. L. Kane, Nucl. Phys. **B182**, 77 (1981); E. Eichten, I. Hinchliffe, K. D. Lane, and C. Quigg, Phys. Rev. D **34**, 1547 (1986).
[3] L. M. Sehgal, Phys. Rev. **183**, 1511 (1969); Phys. Rev. D **4**, 1582(E) (1971); G. L. Kane and R. E. Shrock, in *Proceedings of the Workshop on Intense Medium Energy Sources of Strangeness, Santa Cruz, California, 1983,* edited by T. Goldman, H. E. Haber, and H. F. W. Sadrozinski, AIP Conference Proceedings No. 102 (American Institute of Physics, New York, 1983), p. 123.
[4] Particle Data Group, J. J. Hernández *et al.*, Phys. Lett. B **239**, 1 (1990).
[5] H. B. Greenlee *et al.*, Phys. Rev. Lett. **60**, 893 (1988); S. F. Schaffner *et al.*, Phys. Rev. D **39**, 990 (1989); E. Jastrzembski *et al.*, Phys. Rev. Lett. **61**, 2300 (1988).
[6] R. D. Cousins *et al.*, Phys. Rev. D **38**, 2914 (1988); C. Mathiazhagen *et al.*, Phys. Rev. Lett. **63**, 2181 (1989).
[7] T. Inagaki *et al.*, Phys. Rev. D **40**, 1712 (1989).
[8] T. Akagi *et al.*, following Letter, Phys. Rev. Lett. **67**, 2618 (1991).
[9] The branching ratio for the decay $K_L^0 \to ee\gamma$ was calculated using Eqs. (4) and (5) in L. Bergström, E. Massó, and P. Singer, Phys. Lett. **131B**, 229 (1983), where $\alpha_{K^*} = -0.28$ was quoted from G. D. Barr *et al.*, Phys. Lett. B **240**, 283 (1990); K. E. Ohl *et al.*, Phys. Rev. Lett. **65**, 1407 (1990).
[10] N. M. Kroll and W. Wada, Phys. Rev. **98**, 1355 (1955); T. Miyazaki and E. Takasugi, Phys. Rev. D **8**, 2051 (1973).
[11] G. D. Barr *et al.*, Phys. Lett. B **259**, 389 (1991).